Molecular Pharmacology Fast Forward. Published on April 15, 2008 as doi:10.1124/mol.107.041871
This article has not been copyedited and formatted. The final version may differ from this version.

MOL #41871

Characterization of a Novel Alternative Splice Variant of the Mouse Equilibrative Nucleoside Transporter 1: mENT1Δ11

Kevin R. Robillard[1], Derek B.J. Bone, Jamie S. Park and James R. Hammond

Department of Physiology and Pharmacology, Schulich School of Medicine and Dentistry, University of Western Ontario, London, Ontario, Canada N6A 5C1

Molecular Pharmacology Fast Forward. Published on April 15, 2008 as DOI: 10.1124/mol.107.041871
This article has not been copyedited and formatted. The final version may differ from this version.

Running Title: Equilibrative Nucleoside Transporter Splice Variants

Correspondence to be addressed to:

Dr James R Hammond
Dept of Physiology and Pharmacology
M266 Medical Sciences Building
University of Western Ontario
London, Ontario, N6A 5C1
Canada
Tel: 519-661-3780
Fax: 519-661-3827
Email: jhammo@uwo.ca

# of Text Pages = 35
Tables = 3
Figures = 8
References = 28
Abstract = 246 words
Introduction = 434 words
Discussion = 1373 words

Abbreviations

ENT	Equilibrative Nucleoside Transporter
MEM	Modified Eagle Medium
NBMPR	Nitrobenzylthioinosine
NBTGR	Nitrobenzylthioguanosine
NEM	N-Ethylmaleimide
NMG	n-Methylglucamine
PBS	Phosphate Buffered Saline
PK15-NTD	Pig Kidney epithelial cells 15 - Nucleoside Transport Deficient
PVDF	Polyvinylidene Fluoride
U2-OS	U2-Osteosarcoma

Molecular Pharmacology Fast Forward. Published on April 15, 2008 as DOI: 10.1124/mol.107.041871
This article has not been copyedited and formatted. The final version may differ from this version.

Abstract

Mammalian cells require specific transport mechanisms for the cellular uptake and release of endogenous nucleosides such as adenosine, and nucleoside analogues used in chemotherapy. We have identified a novel splice variant of the mouse equilibrative nucleoside transporter, mENT1, which results from the exclusion of exon 11 during pre-RNA processing. This variant encodes a truncated protein (mENT1Δ11) missing the last three transmembrane domains of the full-length mENT1. The mENT1Δ11 transcript and protein was found to be differentially distributed among tissues relative to full-length mENT1. PK15-NTD (nucleoside transport deficient) cells were transfected with mENT1 or mENT1Δ11 and assessed for nucleoside transport function. No significant differences were observed between the mENT1 and mENT1Δ11 in terms of transport function or inhibitor binding affinity. PK15-mENT1Δ11 transfected cells bound the ENT1 probe [^{3}H]nitrobenzylthioinosine (NBMPR) with high affinity and mediated the cellular accumulation of both [^{3}H]2-chloroadenosine and [^{3}H]uridine. The only significant differences between the mENT1 variants were that mENT1Δ11 could not be photolabelled with [^{3}H]NBMPR, and mENT1Δ11 was insensitive to the transporter-modifying effects of N-ethylmaleimide. These data suggest that the last three transmembrane domains of mENT1 are not necessary for transport activity, but this region does contain the cysteines responsible for the sensitivity of mENT1 to sulfhydryl reagents, and the residues important for covalent modification of the protein with NBMPR. These results provide important guidelines for future mutagenesis studies aimed at elucidating the tertiary structure of the ENT1 protein and the domains involved in inhibitor binding and substrate translocation.

Molecular Pharmacology Fast Forward. Published on April 15, 2008 as DOI: 10.1124/mol.107.041871
This article has not been copyedited and formatted. The final version may differ from this version.

Nucleosides and their therapeutic analogues are hydrophilic molecules which require a system to transport them from the extracellular environment into the cytoplasm of mammalian cells(Zhang et al., 2007;King et al., 2006;Baldwin et al., 2004). In most cell types, this occurs by facilitative diffusion through a family of equilibrative nucleoside transporters (ENTs)(Hyde et al., 2001). The best characterized of this family is ENT1 which is distinguished functionally by its high affinity for the inhibitor nitrobenzylmercaptopurine riboside (nitrobenzylthioinosine, NBMPR)(Hyde et al., 2001). ENT1 mediates the bidirectional transport of a variety of purine and pyrimidine nucleosides, including adenosine which is known to have a variety of endogenous cardiovascular and neural regulatory functions. The ENT1 gene was identified in human and rat tissues in 1997(Yao et al., 1997;Coe et al., 1997;Griffiths et al., 1997), and we obtained the cDNA for the mouse ENT1 in 2000(Kiss et al., 2000). The protein encoded by mENT1 is predicted to consist of 458 amino acids in an 11 transmembrane domain (TM) topology with a large glycosylated extracellular loop joining TM 1 and 2, and a large intracellular loop between TM 6 and 7 (Fig 1). The central intracellular loop is predicted to contain phosphorylation sites for casein kinase II (CK2) and protein kinase C. We, and others, have identified an alternative splice variant of mENT1 that is missing a LYS-GLY in the central intracellular loop and has an arginine in place of a serine in the position (254) preceding the deletion (mENT1a; mENT1.2)(Kiss et al., 2000;Handa et al., 2001). This results in the loss of a potential CK2 phosphorylation site. We have shown that this shorter variant differs from the full-length mENT1 in that it is insensitive to the transporter modifying effects of protein kinase CK2 inhibitors, and has a significantly higher affinity for [^{3}H]NBMPR(Bone et al., 2007).

We have now identified a third mENT1 variant that arises from the skipping of exon 11 during pre-RNA processing, designated mENT1Δ11 (*Genbank accession #EU180577*). This variant was first noted as a 1242 bp RT-PCR product from mouse skeletal muscle when using primers to the open

Molecular Pharmacology Fast Forward. Published on April 15, 2008 as DOI: 10.1124/mol.107.041871
This article has not been copyedited and formatted. The final version may differ from this version.

reading frame of mENT1 (1500 bp) (Genbank accession # AF131212.1). In silica translation of the sequence indicated that the protein encoded by this mRNA would be lacking 102 amino acids from the C-terminal due to the introduction of a frame-shift resulting in a stop codon after position 356. Preliminary studies, presented at the XVth World Congress of Pharmacology, showed that mENT1Δ11 encoded a protein that retained high affinity for [^{3}H]NBMPR. The present study reports on the complete characterization of this novel splice variant.

Molecular Pharmacology Fast Forward. Published on April 15, 2008 as DOI: 10.1124/mol.107.041871
This article has not been copyedited and formatted. The final version may differ from this version.

Methods

Materials

Culture flasks were purchased from Becton Dickinson Bio-sciences (Franklin Lakes, New Jersey). Modified Eagle Medium (MEM), sodium pyruvate, non-essential amino acids, Geneticin® (G418), LipofectAMINE 2000™, penicillin / streptomycin solution, trypsin / EDTA solution, and culture-grade phosphate buffered saline (PBS) were purchased from GIBCO/BRL (Burlington, Ontario, Canada). N-ethylmaleimide (NEM), 2-chloroadenosine, dipyridamole (2,6-bis(diethanolamino)-4,8-dipiperidino-pyridmido-[4,5-d]pyrimidine), NBMPR, nitrobenzylthioguanosine (NBTGR, S-4-nitrobenzyl)-6-thioguanosine), rabbit polyclonal anti-FLAG antibody, goat anti-rabbit antibody conjugated to horseradish peroxidase, p3XFLAG-CMV10 vector, protease inhibitor cocktail (4-(2-aminoethyl)benzenesulfonyl fluoride, pepstatinA, E-64, bestatin, leupeptin, and aprotinin), and mRNA purification kits were purchased from Sigma-Aldrich (Oakville, Ontario, Canada. The anti-ENT1 antibody (ENT1 (K-15); affinity purified polyclonal), raised to the C-terminal end of the central intracellular loop of ENT1 (amino acids 250-300), was from Santa Cruz Biotechnology. Draflazine (2-(aminocarbonyl)-4-amino-2,6-dichlorophenyl)-4-[5,5-bis(4-fluorophenyl)pentyl]-1-piperazine acetamide 2HCl) was acquired from Janssen Research Foundation (Beerse, Belgium). Dilazep ((N,N'-bis[3-(3,4,5-trimeth-oxybenzo-yloxy)propyl]-homo-piperazine) was provided by Asta Werke (Frankfurt, Germany). [^{3}H]NBMPR (5.5 – 20.1 Ci/mmol), [^{3}H]2-chloroadenosine (9.1 Ci/mmol), and [^{3}H]water (1 mCi/g) were purchased from Moravek Biochemicals (Brea, California, USA). Oligonucleotide primers were purchased from Sigma-Genosys (Oakville, Ontario, Canada), and all restriction enzymes were from Fermentas International Inc (Burlington, Ontario, Canada). Platinum Taq polymerase, Superscript First-Strand Synthesis System for RT-PCR, Pure-link Gel-Extraction Kit, DH5α E.*coli* , the Benchmark

Molecular Pharmacology Fast Forward. Published on April 15, 2008 as DOI: 10.1124/mol.107.041871
This article has not been copyedited and formatted. The final version may differ from this version.

Prestained Protein Ladder, and the pcDNA3.1TOPO kit were purchased from Invitrogen (Burlington, Ontario, Canada). Mini-prep Plasmid DNA kits were obtained from Qiagen (Mississauga, Ontario, Canada), and cloning rings were purchased from Bel-Art Scienceware (Pequannock, New Jersey, USA). U2-osteosarcoma (U2-OS) cells were a gift from Dr David Litchfield (Biochemistry, University of Western Ontario, London, Canada) and the PK15-NTD cells used for creating the stable mENT1 cell lines were provided by Dr Ming Tse (Johns Hopkins University, Baltimore, USA).

Plasmid Generation

mENT1 and mENT1Δ11 were obtained from mouse skeletal muscle tissue by RT-PCR using Platinum Taq polymerase and primers complementary to the 5' and 3' termini of the open reading frame of mENT1 (5'mENT1, 3'mENT1-Kpn1; Table 1). PCR conditions were: initial activation for 5 min at 95°C, followed by 35 cycles of 30 sec at 95°C, 30 sec at 55°C, and 30 sec at 72°C, and a final 10 min elongation at 72°C. The PCR products were ligated into the multiple cloning site of pcDNA3.1 using the TOPO cloning procedure. All constructs were sequenced in both directions (Robarts Research Institute - Sequencing Facility, London, Canada) using the Taq BigDye Terminator Cycle Sequencing kit in an automated ABI PRISM Model 377 Version 3.3 DNA sequencer. The nucleotide sequences were translated and transmembrane topology predictions made using the Tmpred software (www.ch.embnet.org /software/TMPRED_form.html).

To generate plasmids encoding mENT1 or mENT1Δ11 with an N-terminal FLAG epitope tag (DYKYYYD), pcDNA3.1-mENT1 and pcDNA3.1-mENT1Δ11 were used as templates for PCR with primers containing the appropriate restriction enzyme cut sites (5'HindIII-mENT1 and 3'mENT1-Kpn1; Table 1) for ligation into the p3XFLAG-CMV10 vector. PCR products were separated on a 1.2% agarose gels containing ethidium bromide, cut with the appropriate restriction enzyme and ligated into p3XFLAG-CMV10. DH5α sub-cloning efficiency *E.coli* cells were

Molecular Pharmacology Fast Forward. Published on April 15, 2008 as DOI: 10.1124/mol.107.041871
This article has not been copyedited and formatted. The final version may differ from this version.

transformed with the plasmid constructs using 42°C heat shock according to manufacturer's (Invitrogen) protocol, and plated on Luria-Bertani broth-agar plates containing 100µg/ml ampicillin. Plasmid DNA was isolated from transformed DH5α cells using according to manufacturer's (Qiagen) protocols.

Stable Transfections

PK15-NTD (Nucleoside Transport Deficient) cells were transfected with pcDNA3.1-mENT1, pcDNA3.1-mENT1Δ11, p3XFLAG-CMV10-mENT1, or p3XFLAG-CMV10-mENT1Δ11 using Lipofectamine 2000™. The ratio of DNA:Lipofectamine 2000™ was 1:3, using approximately 4.0 µg of plasmid DNA. Transfected cells were selected based on survival in 500 µg/ml G418 and individual cell colonies were isolated after limiting dilution of the surviving cells. The PK15-mENT1 and PK15-mENT1Δ11 cell lines were maintained at 37°C in a 5% CO_2 humidified atmosphere in vented tissue culture flasks containing MEM supplemented with 10% (v/v) bovine growth serum (BGS), 100 units of penicillin, 100µg/ml of streptomycin, 0.1mM non-essential amino acids, 1mM sodium pyruvate and 300 µg/ml of G418 (*30*). mRNA was collected from each cell clone and tested for the presence of the respective mENT1 or mENT1Δ11 transcript by RT-PCR using primers spanning the open reading frame of mENT1 (Table 1).

Immunoblotting of Transiently-Transfected U2-OS Cells

Transient transfection of U2-OS cells with p3xFLAG-mENT1 and p3xFLAG-mENT1Δ11 was conducted to confirm that the encoded proteins were being properly expressed. U2-OS cells were grown in Dulbecco's Modified Eagle medium with 10% BGS (v/v), 100 units of penicillin and 100µg/ml streptomycin. p3XFLAG-mENT1, p3XFLAG-mENT1Δ11 or empty p3XFLAG-vector (25µg / 175cm^2 flask) was diluted in TE buffer (10mM TRIS-HCl, 1mM EDTA, pH 7.3) containing 0.25mM

$CaCl_2$. This DNA+$CaCl_2$ solution was then added drop wise to bubbling 2x concentrated HEPES buffered saline (280mM NaCl, 50mM HEPES, 1.5mM Na_2HPO_4, pH=7.05). The mixture was incubated at room temperature for 20 min to form a calcium precipitate and was then added to 40% confluent U2-OS cells in 175cm^2 flask. The cells were incubated with the precipitate overnight (~16 hr) at 37°C in a 5% CO_2 atmosphere, then washed with PBS and fresh media added. Cells were harvested 48 hrs after initial transfection for the preparation of cell membranes.

U2-OS cells expressing p3XFLAG-mENT1, p3XFLAG-mENT1Δ11 or empty vector were removed from their flasks with 0.05% Trypsin/EDTA and re-suspended in 5mM sodium phosphate buffer (5mM Na_2HPO_4, pH 7.2) containing a mammalian protease inhibitor cocktail. Cells were incubated in the lysis buffer for 30 min on ice and were subjected to sonication using a Sonic Dismembrator Model 150 (Fisher Scientific, New Jersey, New York) (setting 5, 30 s x 3). Cell/membrane suspensions were then centrifuged (4°C, 3000xg x 30 min) to pellet nuclei and unbroken cells. The supernatant was centrifuged (4°C) for 1 h at 30,000xg, and the pelleted membranes suspended in 5 mM sodium phosphate lysis buffer containing protease inhibitor cocktail. Bradford colormetric protein assays were performed on each membrane preparation to quantify total protein yield.

For immunoblotting, 20 µg of membrane protein was denatured for 2 min at 100°C in SDS sample buffer (0.5M Tris-Cl pH6.8, 30% glycerol, 10% SDS, 0.6M DTT, 0.0012% bromophenol blue) and subjected to SDS-polyacrylamide gel electrophoresis on a 12% acrylamide gel. Samples were then transferred to polyvinylidene fluoride (PVDF) membranes using a Trans-Blot SD Semi-Dry Transfer Cell (Biorad, Hercules, CA, USA) . The PVDF membranes were blocked overnight with 5% skim milk in TBS-T buffer (0.5mM TRIS, 13.8mM NaCl, 2.7mM KCl and 0.01% Tween-20). After 3 washes of 10 min each in fresh TBS-T buffer, PVDF membranes were incubated with primary polyclonal rabbit anti-FLAG antibody for two hrs at room temperature (1:1000 dilution, 3%

Molecular Pharmacology Fast Forward. Published on April 15, 2008 as DOI: 10.1124/mol.107.041871
This article has not been copyedited and formatted. The final version may differ from this version.

skim milk in TBS-T buffer). After three washes of 10 min each with TBS-T buffer, PVDF membranes were incubated with polyclonal goat anti-rabbit secondary antibody conjugated to horseradish peroxidase (1:5000 dilution, 3% skim milk in TBS-T buffer) for 1 hr at room temperature. Antigen reactivity was detected using LumiGLO™ Chemiluminescent Substrate (Upstate Cell Signaling Solutions, Temecula, CA). Molecular mass was determined by comparing R_f values against a Benchmark Prestained Protein Ladder.

[^{3}H]NBMPR Binding

Cells were removed from flasks by trypsinization (0.05% v/v trypsin / 0.53 mM EDTA, 5 min, 37 °C) and diluted with their respective media containing 10% (v/v) BGS and collected by centrifugation. Cell pellets were washed once by resuspension/centrifugation in isotonic n-methyl-glucamine(NMG) buffer (pH 7.25) containing 140mM NMG, 5mM KCl, 4.2mM $KHCO_3$, 0.36mM K_2HPO_4, 0.44mM KH_2PO_4, 10mM HEPES (sodium free), 0.5mM $MgCl_2$ and 1.3mM $CaCl_2$, and then resuspended in this buffer for subsequent assays. Cell concentrations were determined routinely using a haemocytometer. In some cases, cells were incubated for 30 min on ice with 300 μM NEM, and then washed 4 times with NMG buffer to remove unreacted NEM, prior to use in the binding assays.

PK15-NTD, PK15-mENT1 or PK15-mENT1Δ11 (± 3XFLAG) cells, and isolated membranes prepared as described above, were incubated with [^{3}H]NBMPR using procedures that we have described previously(Bone et al., 2007). Nonspecific binding of [^{3}H]NBMPR was defined as that seen in the presence of 10μM NBTGR. This concentration of NBTGR is 1000-fold greater than its K_I for inhibition of [^{3}H]NBMPR binding to ENT1(Hammond, 1991). Specific binding of [^{3}H]NBMPR was calculated as total minus non-specific binding. Non-linear regression analysis (Graphpad Prism v 4.0) was used to fit rectangular hyperbolic curves to the site-specific binding of [^{3}H]NBMPR

Molecular Pharmacology Fast Forward. Published on April 15, 2008 as DOI: 10.1124/mol.107.041871
This article has not been copyedited and formatted. The final version may differ from this version.

plotted against the free [^{3}H]NBMPR concentration at steady-state.

[^{3}H]NBMPR Photoaffinity Labelling

Membranes prepared from PK15-mENT1 and PK15–mENT1Δ11 cells were photolabelled with [^{3}H]NBMPR as we have described previously(Hammond and Johnstone, 1989). Briefly, membranes were incubated with 5 nM [^{3}H]NBMPR for 40 min at room temperature to allow for steady-state binding. Dithiothreitol (10 mM final conc.) was then added and the mixture placed in a Petri dish on ice and exposed to 45 s of UV light (repeated 3 times with 1 min cooling on ice between UV exposures) from a 200W mercury-arc lamp at a distance of 4 cm, with constant stirring with a magnetic stir bar. Membranes were washed three times in 5mM sodium phosphate buffer by centrifugation at 10000 x g for 3 min, and suspended in Laemmli's SDS-PAGE buffer and incubated at 50°C for 5 min to denature protein. Solubilized membranes were electrophoresed on a 6% SDS-polyacrylamide stacking gel and 5-15% gradient SDS-polyacrylamide separating gel. Gels were then fixed in 5% acetic acid and each gel lane cut into 2mm slices for analysis of [^{3}H]content. Radioactivity was plotted against the distance travelled (mm) in the gel and was compared to the reference protein ladder to determine approximate molecular mass of the radiolabelled proteins.

[^{3}H]Substrate Uptake

To compare the kinetic properties of substrate translocation by mENT1Δ11 and mENT1, [^{3}H]2-chloroadenosine and [3H]uridine uptake was examined using methods described previous by our laboratory (Bone et al., 2007;Stolk et al., 2005) . Briefly, cells were incubated with [^{3}H]substrate (± test inhibitors) in 1.5 ml microcentrifuge tubes over a 200 µl layer of 84% silicone/ 16% light mineral oil. Uptake reactions were terminated by centrifugation of the cells through the

Molecular Pharmacology Fast Forward. Published on April 15, 2008 as DOI: 10.1124/mol.107.041871
This article has not been copyedited and formatted. The final version may differ from this version.

oil layer followed by digestion of the cell pellet in 1 M NaOH. Transporter-mediated uptake was defined as the total cell accumulation of radiolabel minus the amount of cell associated radiolabel in the presence of a supramaximal inhibitory concentration (10 μM) of the ENT inhibitors NBTGR and dipyridamole. In some cases, cells were incubated with 300 μM NEM for 30 min on ice and then washed extensively with NMG buffer (4 times) prior to assessment of [^{3}H]2-chloroadenosine uptake.

Tissue Distribution of mENT1 and mENT1Δ11

To examine the relative endogenous distribution of mRNA transcript and protein corresponding to mENT1 and mENT1Δ11, a range of tissues (heart, lungs, liver, kidney, brain, pancreas, thymus, skeletal muscle, spleen and testes) from three male C57BL/6 mice were isolated and either digested in guanidinium isothiocyanate buffer(4.2 M, containing 25mM sodium citrate, 1mM EDTA and 0.007% β-mercaptoethanol, pH 7.0) for RNA extraction, or snap frozen in liquid nitrogen for subsequent immunoblotting. Total RNA was isolated using standard phenol-chloroform extraction methods, and mRNA was purified from total RNA using the Sigma mRNA purification kit™. cDNA was generated from isolated mRNA then target transcripts amplified using Platinum Taq polymerase™ and primers spanning the full coding region of mENT1 (5'mENT1 and 3'mENT1-Kpn1; Table 1). The 3' primer is designed to anneal to a region located near the end of exon 12, which is present in both the mENT1 and mENT1Δ11, allowing amplification of both transcripts within a single reaction. PCR products were then electrophoresed on a 2% agarose gel with ethidium bromide for approximately 1 hr (100mV, room temperature). Gels were photographed on a digital Alpha Innotech imaging system.

For immunoblotting, frozen tissue was homogenized in 3 ml/g RIPA buffer containing a protease inhibitor cocktail. Protein samples (100 μg) were denatured for 2 min at 100°C in SDS

Molecular Pharmacology Fast Forward. Published on April 15, 2008 as DOI: 10.1124/mol.107.041871
This article has not been copyedited and formatted. The final version may differ from this version.

sample buffer and subjected to SDS-polyacrylamide gel electrophoresis on a 12.5% gel. Samples were then transferred to PVDF membranes, blocked with 5% skim milk in TBS-T for 2 hours at room temperature, then immunolabeled with goat anti-ENT1 polyclonal antibody diluted 1:200 in blocking solution at 4°C overnight (~16h). Membranes were washed in TBS-T and subsequently incubated with donkey anti-goat secondary antibody conjugated to horseradish peroxidase (1:2000 dilution) for 2 hours at room temperature. Following an additional wash, immunoreactivity was detected using LumiGLO™ Chemiluminescent Substrate. Molecular mass was determined by comparing R_f values against a Benchmark Prestained Protein Ladder. Specificity of the ENT1 antibody was confirmed by its lack of immunoreactivity to membranes prepared from PK15NTD cells which do not express ENT1.

To investigate the existence of a human ENT1 splice variant analogous to mENT1Δ11, human major tissue cDNA panel I and II (Biochain Institute, Hayward, CA, USA) isolated from brain, heart, kidney, liver, lung, pancreas, placenta, spleen and skeletal muscle were screened by PCR, using the conditions described above, with primers designed to span the open reading frame of hENT1 (5'hENT1 and 3'hENT1;Table 1). mRNA was also isolated from human umbilical microvascular endothelial cells and human U2-OS cells and screened for ENT1Δ11 like transcripts as described above.

Statistical and Data Analyses

All data were analyzed using Lotus 1-2-3 1997 ™ and[^{3}H]NBMPR and [^{3}H]substrate uptake data were fit to both a one-site and two-site model (Graphpad Prism 4.0, San Diego, California, USA) and each curve was analyzed for accuracy of fit to the data set by the F-test ($P<0.05$). Data are represented as mean ± SEM from replicate independent experiments conducted in duplicate. Differences were assessed by paired or unpaired Student's t-test, as appropriate, with $P<0.05$ considered significant.

Molecular Pharmacology Fast Forward. Published on April 15, 2008 as DOI: 10.1124/mol.107.041871
This article has not been copyedited and formatted. The final version may differ from this version.

Results

mENT1Δ11 Structure

The predicted membrane topology of mENT1Δ11 is shown in Fig. 1. The amino acid sequence corresponds to the variant of mENT1 with an arginine at position 254 (mENT1a; Genbank accession # AF131212.1). Examination of the mENT1 gene indicates that mENT1Δ11 arises from the splicing of the 3' end of exon 10 to the 5' splice site of exon 12. This results in a frame-shift at the splice point leading to a premature stop codon after the translation of five unique C-terminal amino acids (tryptophan, glutamate, glutamine, threonine and serine). mENT1Δ11 is predicted to have 9 TM domains and cytoplasmic C- and N-termini.

To confirm that ENT1Δ11 did indeed encode a truncated protein. Membranes prepared from U2-OS cells transiently transfected with either p3XFLAG-mENT1, p3XFLAG-mENT1Δ11, or the empty p3XFLAG-vector were subjected to electrophoresis and immunoblotting with polyclonal rabbit anti-FLAG antibody. Bands corresponding to the predicted 33 kDa p3XFLAG-mENT1Δ11 and the 48 kDa p3XFLAG-mENT1 were detected, indicating that these proteins were expressed and were of the expected size (Fig. 2).

Tissue Distribution

RT-PCR was performed using cDNA prepared from mRNA isolated from several mouse tissues. mENT1Δ11 transcript was detected as a ~1250 bp band compared to full-length mENT1(~1500 bp) on 2% agarose gels stained with ethidium bromide. These studies showed that mENT1Δ11 expression is ubiquitous, similar to the distribution of mENT1, appearing in brain, heart, kidney, liver, lung, pancreas, skeletal muscle, spleen, thymus and testes.

Molecular Pharmacology Fast Forward. Published on April 15, 2008 as DOI: 10.1124/mol.107.041871
This article has not been copyedited and formatted. The final version may differ from this version.

However, there were distinct differences in the relative ratio of mENT1 to mENT1Δ11 is some tissues (Fig. 3). Tissues with a higher relative ratio of mENT1Δ11 to mENT1 included thymus, brain, skeletal muscle and pancreas. The 1250 bp bands from skeletal muscle and brain were extracted and sequenced to confirm their identity as mENT1Δ11.

Examination of a number of human tissues and cell-lines by RT-PCR revealed a hENT1 PCR product of approximately 1500 base pairs in all tissues and cells tested. There was no evidence of a smaller PCR product analogous to mENT1Δ11 in any of the human tissues examined (data not shown).

To confirm that the mENT1Δ11 protein was actually being expressed in mouse tissues, mENT1 antibody reactivity was assessed in mouse brain, testis, liver and pancreas. Brain and testis immunoblots had bands at ~45-50 kDa and ~35-40 kDa, which correspond to the expected sizes of the full-length mENT1 and mENT1Δ11 respectively. However, liver had predominantly the 50 kDa mENT1 and pancreas showed predominantly the 40 kDa mENT1Δ11. The double band in liver at the 50 kDa range likely represents multiple glycosylation states of mENT1((Vickers et al., 1999).

[^{3}H]NBMPR Binding

PK15-mENT1 and PK15–mENT1Δ11 cells bound [^{3}H]NBMPR with similar affinity (K_d < 0.2 nM) to more than 500,000 sites per cell (Table 2; Fig 4A). The PK15-3xFLAG-mENT1 cells also bound [^{3}H]NBMPR to a single class of site with a K_d of 0.15 ± 0.01 to a maximum of 520000 ± 110000 sites per cell (Fig 4B). However, [^{3}H]NBMPR binding to the PK15-3xFLAG-mENT1Δ11 cells fit best (2 independent cell clones tested) to a two site model with 550000 ± 150000 sites/cell having an affinity of 1.9 ± 0.8 nM, and an additional 135000 ± 40000 sites/cell

Molecular Pharmacology Fast Forward. Published on April 15, 2008 as DOI: 10.1124/mol.107.041871
This article has not been copyedited and formatted. The final version may differ from this version.

having an affinity of 0.021 ± 0.005 nM (Fig 4B; Table 2). The untransfected PK15-NTD cell line showed no apparent specific binding of [^{3}H]NBMPR (data not shown).

Photolabelling of PK15-mENT1 cell membranes with [^{3}H]NBMPR led to a distinct radiolabelled band on SDS-PAGE gels in the 48 kDa range, which is the expected size of the mENT1 protein (Fig 5). There was also an additional peak seen at approximately 100 kDA, possibly representing mENT1 dimers. PK15-mENT1Δ11 cell membranes were treated with [^{3}H]NBMPR and exposed to uv light in parallel with the PK15-mENT1 membranes. The expected size of mENT1Δ11 protein was 33 kDa; however, no distinct radiolabelled peaks were observed on gels of the PK15-mENT1Δ11 proteins after exposure to [^{3}H]NBMPR (Fig. 5), even though these same isolated membranes bound [^{3}H]NBMPR with high affinity in reversible binding assays (data not shown).

[^{3}H]Substrate Uptake

PK15-mENT1Δ11 cells accumulated 10μM [^{3}H]2-chloroadenosine (a purine substrate for ENT1) with an initial rate of transporter-mediated uptake of 0.49 ± 0.10 pmol/μl/s, to a maximum intracellular concentration of 23 ± 3 μM (Fig 6A). This rate of uptake was similar to that discerned previously for mENT1a transfected PK15 cells(Bone et al., 2007). To determine whether there was a change in permeant selectivity in the mENT1Δ11 variant, the uptake of the pyrimidine substrate uridine was also examined. PK15-mENT1 and PK15-mENT1Δ11 cells accumulated 100 μM [^{3}H]uridine in a transporter-dependent manner with initial rates of 2.1 ± 0.3 and 4.4 ± 0.7 pmol/μl/s, respectively (Fig 6B). Based on these initial time course studies, an incubation time of 15 sec was selected for the assessment of the rate of uptake of a range of concentrations of [^{3}H]2-chloroadenosine. PK15-mENT1Δ11 cells transported 2-chloroadenosine

Molecular Pharmacology Fast Forward. Published on April 15, 2008 as DOI: 10.1124/mol.107.041871
This article has not been copyedited and formatted. The final version may differ from this version.

with similar affinity (K_m = 66 μM) as the PK15-mENT1 cells (K_m = 43 μM). Likewise, there was no significant difference in the V_{max} of [^{3}H]2-chloroadenosine transport in the two cell lines (3.5 ± 1.1 pmol/μl/s and 4.4 ± 1.7pmol/μl/s for the PK15-mENT1Δ11 and PK15- mENT1a cells, respectively). (Fig. 6C). Similar studies, using a 5 sec incubation period, conducted with the PK15-3xFLAG-mENT1 and PK15–3xFLAG-mENT1Δ11 cells revealed K_m values of 44 ± 18 and 43 ± 11 μM respectively and V_{max} values of 17 ± 4 and 19 ± 3 pmol/μl/s respectively.

Several known ENT1 inhibitors (NBMPR, dilazep, draflazine and dipyridamole) and endogenous substrates (adenosine and uridine) were assessed for their abilities to block [^{3}H]2-chloroadenosine uptake by PK15-mENT1 and PK15-mENT1Δ11 cells (Fig. 7). The pseudo-Hill coefficients for all inhibitors were not significantly different from -1 and therefore the Cheng-Prusoff equation(Cheng and Prusoff, 1973) was used to calculate K_I values. NBMPR was the most effective inhibitor with a K_I of 0.5 ± 0.2 nM and 0.9 ± 0.3 nM for PK15-mENT1 and PK15–mENT1Δ11, respectively followed by draflazine, dilazep and dipyridamole. Adenosine was approximately 50 times more effective at inhibiting [^{3}H]2-chloroadenosine uptake than was uridine in both the PK15-mENT1 (4 ± 2 μM, 200 ± 29 μM) and the PK15-mENT1Δ11 (3 ± 1 μM, 165 ± 71 μM), respectively. There were no significant differences in K_I values (Student's paired t-test, $P<0.05$) for PK15-mENT1Δ11 compared to PK15-mENT1 for any of the inhibitors or substrates tested (Table 2).

Effect of NEM

Treatment of PK15-3xFLAG-mENT1 with 300 μM NEM for 30 min on ice increased both the Kd and Bmax of [^{3}H]NBMPR binding to 3xFLAG-mENT1 compared to untreated control cells. In contrast, NEM affected only the higher affinity component of the biphasic [^{3}H]NBMPR binding to the PK15-3xFLAG-mENT1Δ11 cells. NEM also increased both the K_m and V_{max} of

Molecular Pharmacology Fast Forward. Published on April 15, 2008 as DOI: 10.1124/mol.107.041871
This article has not been copyedited and formatted. The final version may differ from this version.

[^{3}H]2-chloroadenosine uptake by the full-length mENT1, but had no significant effect on the mENT1Δ11 variant (Fig. 8, Table 3). Similar uptake data (±NEM) were obtained using PK15-NTD cells transfected with either the 3XFLAG-tagged or non-FLAG-tagged versions of mENT1 and mENT1Δ11 (data not shown).

Molecular Pharmacology Fast Forward. Published on April 15, 2008 as DOI: 10.1124/mol.107.041871
This article has not been copyedited and formatted. The final version may differ from this version.

Discussion

The data presented in this report indicate that the last three transmembrane domains of mENT1 are not required for membrane expression, translocation activity or ligand binding of mENT1. No differences were noted between the full-length mENT1 and the truncated mENT1Δ11 in terms of substrate or inhibitor affinity. mENT1 and mENT1Δ11 are both widely expressed but differ in their relative levels of expression in a number of tissues, suggesting that the expression of the truncated variant is regulated differently than that of the full-length ENT1. Of the tissues examined, brain, thymus, skeletal muscle and pancreas have more mENT1Δ11 transcript when compared to the full-length mENT1. In contrast, liver shows mostly the full-length mENT1 transcript. A compatible profile of mENT1 immunoreactivity was also seen in these tissues, with brain and testis having both a ~45-50 kDa band and a 35-40 kDa band, while liver showed only the 45-50 kDa band and pancreas had only the 35-40 kDa variant. The fact that the mRNA profile does not exactly match the protein ratio of mENT1:mENT1Δ11 in some tissues (e.g. testis) may be due to differences in mRNA translation rates or stability of the two transcripts, or may reflect an age related difference in the expression of the mENT1 variants (the western blots and PCR experiments were done on tissues from different animals). The slight differences in size of the mENT1 bands between tissues is likely due to differences in the extent of glycosylation. In general, these molecular masses are a bit lower than the predicted sizes of mENT1 (50 kDa) and mENT1Δ11 (40 kDa), but are similar to those noted in other studies for photoaffinity-labelled mENT1 (Hammond and Johnstone, 1989). The tissues with high levels of mENT1Δ11 all tend to be highly metabolically active tissues, and thus one could speculate that the mENT1Δ11 variant may be expressed in response to an enhanced requirement for nucleoside salvage to support the increased metabolic activity. Unfortunately, there is

Molecular Pharmacology Fast Forward. Published on April 15, 2008 as DOI: 10.1124/mol.107.041871
This article has not been copyedited and formatted. The final version may differ from this version.

insufficient functional data available in the literature at this time to confirm that these tissues actually do have enhanced nucleoside transport capacity; most studies on nucleoside transport are conducted in isolated cell lines.

The only functional differences noted between mENT1 and mENT1Δ11 were that: 1) mENT1Δ11 cannot bind [^{3}H]NBMPR irreversibly upon exposure to UV light, and 2) [^{3}H]2-chloroadenosine uptake by mENT1Δ11 is insensitive to the sulfhydryl reagent NEM. The inability of [^{3}H]NBMPR to photolabel mENT1Δ11 suggests that the loss of this C-terminal region of mENT1 removes the residue that NBMPR normally cross-links to, or that a critical residue has shifted position as a result of the structural rearrangement of the protein that likely occurs in the truncated variant. Given that mENT1Δ11 retains the ability to bind [^{3}H]NBMPR reversibly with high affinity, and the previous finding that the site of uv light induced covalent attachment of [^{3}H]NBMPR to hENT1 is in the N-terminal half of the protein(Kwong et al., 1993), we would argue that the loss of the last three transmembrane domains of mENT1 leads to a conformation change that prevents covalent attachment of the [^{3}H]NBMPR to elements of its binding pocket in the N-terminal part of the protein. It is generally believed that it is the S-nitrobenzyl group of NBMPR that is photoactivated upon exposure to UV light, and hence the amino acid residue involved in the photoaffinity labelling is likely proximal to the mENT1 region that binds the S-nitrobenzyl moiety of NBMPR(Shi et al., 1984;Young et al., 1983;Paterson and Oliver, 1971;Zhu et al., 2003).

We noted biphasic saturation profiles for [^{3}H]NBMPR binding in some of the models tested in this study. In other cases, while not obviously biphasic, [^{3}H]NBMPR binding had Hill coefficients of less than unity. These results likely reflect two populations of [^{3}H]NBMPR binding proteins in these heterologous expression models, possibly representing those present at the cell surface (high affinity) and others in intracellular compartments (lower affinity). Similar

biphasic [^{3}H]NBMPR binding profiles have been described in Ehrlich ascites tumour cells(Vyas et al., 2002) , endothelial cells(Hammond and Archer, 2004) and BeWo cells(Boumah et al., 1992).

Treatment of PK15-mENT1 cells with NEM increased the high-affinity binding of NBMPR and enhanced the uptake of 2-chloroadenosine by mENT. In contrast, NEM had no affect on these parameters in the PK15-mENT1Δ11 cells. There are four cysteine residues in theTM9 - C terminal region of the mENT1. These cysteines are clearly not critical for transporter function since their loss from mENT1Δ11 did not affect 2-chloroadenosine or uridine uptake or [^{3}H]NBMPR binding. These results are compatible with a previous study on the effect of NEM on NBMPR binding to mouse Ehrlich ascites tumour cells where we found that 100 μM NEM enhanced the ability of the nucleoside substrates uridine, adenosine and deoxyadenosine to inhibit NBMPR binding(Vyas et al., 2002). Since treatment of the cells with NEM was conducted on ice, the NEM-induced increase in ENT1 activity was not likely due to trafficking of ENT1 protein from intracellular compartments to the plasma membrane. Rather, NEM treatment may be leading to the activation of cryptic transporters that already exist in the plasma membrane. A similar increase in ENT1-mediated nucleoside uptake, in the absence of increased plasma membrane ENT1 protein, was reported recently by Coe and colleagues in response to protein kinase C activation (Coe et al., 2002). Regardless of mechanism, this enhancement by NEM is lost in the mENT1Δ11 variant suggesting that one or more of the four cysteines in the C-terminal region of mENT1 are involved in this effect. Thus we propose that the TM9 to C-terminus region of the transporter is functionally-linked to, but not directly part of, the [^{3}H]NBMPR binding site and substrate translocation mechanism.

Little is known about the tertiary structure of ENT1. A number of studies have implicated the TM3-TM6 region in the binding of NBMPR and the translocation of substrates(Baldwin et al.,

2004). Regions outside of TM3-TM6 have also been shown to impact on ligand binding to ENTs, but almost all of the studies implicating specific regions/residues in ligand binding and transporter function have focussed on amino acids upstream of TM9(Visser et al., 2007;Visser et al., 2005b). The exceptions are a study showing that Arg404 of the Leishmania donovani nucleoside transporter LdNT1.1 (corresponding to Arg369 in TM9 of hENT1) is important for function and substrate specificity(Valdes et al., 2006), and a study showing that Leu442 in TM11 of hENT1 is important for substrate selectivity(Visser et al., 2005a). These results are difficult to reconcile with fact that mENT1Δ11, which is missing TM9-TM11 transports both the purine nucleoside 2-chloroadenosine and the pyrimidine nucleoside uridine as effectively as the full-length mENT1. It is possible that a more detailed analysis of the substrate specificity of mENT1Δ11 will reveal subtle differences relative to mENT1. Interestingly, mutation of Phe334 in TM8 of hENT1 to tyrosine dramatically enhanced the turnover rate (molecules/s) of the ENT1 transporter(Visser et al., 2007), reminiscent of the effect of NEM on 2-chloroadenosine uptake seen in the present study. These results suggest that the TM8 is conformationally linked to the substrate translocation mechanism in TMs 4 and 5, and cysteine residues in the TM9-TM11 region may impact on this interaction.

The ability of ENT proteins to function in spite of a major C-terminal deletion is not unique to the mouse ENT1. An ENT2 splice variant lacking the last four TM domains has been identified in rabbit (rbENT2a)(Wu et al., 2005). rbENT2a was shown to be expressed to the plasma membrane and remained functional, with some slight differences in substrate affinity and inhibitor sensitivities.

In summary, we have shown that truncation of the mENT1 protein in the intracellular loop prior to TM9 does not affect the expression or function of the transporter upon stable transfection in PK15-NTD cells. The inability of the truncated mENT1Δ11 variant to be

Molecular Pharmacology Fast Forward. Published on April 15, 2008 as DOI: 10.1124/mol.107.041871
This article has not been copyedited and formatted. The final version may differ from this version.

covalently labelled with [^{3}H]NBMPR and its reduced sensitivity to the sulfhydryl reagent NEM, highlight potential interactions between the TM9-TM11 C-terminal end of the protein and the TM3-TM6 region implicated in substrate and inhibitor binding. These results provide important guidelines for future mutagenesis studies aimed at elucidating the tertiary structure of the ENT1 protein and the domains involved in inhibitor binding and substrate translocation.

Reference List

Baldwin SA, Beal P R, Yao S Y, King A E, Cass C E and Young J D (2004) The Equilibrative Nucleoside Transporter Family, SLC29. *Pflugers Arch* **447**:735-743.

Bone DB, Robillard K R, Stolk M and Hammond J R (2007) Differential Regulation of Mouse Equilibrative Nucleoside Transporter 1 (MENT1) Splice Variants by Protein Kinase CK2. *Mol Membr Biol* **24**:294-303.

Boumah CE, Hogue D L and Cass C E (1992) Expression of High Levels of Nitrobenzylthioinosine-Sensitive Nucleoside Transport in Cultured Human Choriocarcinoma (BeWo) Cells. *Biochem J* **288**:987-996.

Cheng Y and Prusoff W H (1973) Relationship Between the Inhibition Constant (K1) and the Concentration of Inhibitor Which Causes 50 Per Cent Inhibition (I50) of an Enzymatic Reaction. *Biochem Pharmacol* **22**:3099-3108.

Coe I, Zhang Y, McKenzie T and Naydenova Z (2002) PKC Regulation of the Human Equilibrative Nucleoside Transporter, HENT1. *FEBS Lett* **517**:201-205.

Coe IR, Griffiths M, Young J D, Baldwin S A and Cass C E (1997) Assignment of the Human Equilibrative Nucleoside Transporter (HENT1) to 6p21.1-P21.2. *Genomics* **45**:459-460.

Griffiths M, Beaumont N, Yao S Y M, Sundaram M, Boumah C E, Davies A, Kwong F Y P, Coe I, Cass C E, Young J D and Baldwin S A (1997) Cloning of a Human Nucleoside

Transporter Implicated in the Cellular Uptake of Adenosine and Chemotherapeutic Drugs. *Nature Med* **3**:89-93.

Hammond JR (1991) Kinetic Analysis of Ligand Binding to the Ehrlich Cell Nucleoside Transporter: Pharmacological Characterization of Allosteric Interactions With the [^{3}H]Nitrobenzylthioinosine Binding Site. *Mol Pharmacol* **39**:771-779.

Hammond JR and Archer R G (2004) Interaction of the Novel Adenosine Uptake Inhibitor 3-[1-(6,7-Diethoxy-2-Morpholinoquinazolin-4-Yl)Piperidin-4- Yl] -1,6-Dimethyl - 2,4(1*H*,3*H*) - Quinazolinedione Hydrochloride (KF24345) With the *Es* and *Ei* Subtypes of Equilibrative Nucleoside Transporters. *J Pharmacol Exp Ther* **308** :1083-1093.

Hammond JR and Johnstone R M (1989) Solubilization and Reconstitution of a Nucleoside-Transport System From Ehrlich Ascites-Tumour Cells. *Biochem J* **262**:109-118.

Handa M, Choi D, Caldeiro R M, Messing R O, Gordon A S and Diamond I, I (2001) Cloning of a Novel Isoform of the Mouse NBMPR-Sensitive Equilibrative Nucleoside Transporter (ENT1) Lacking a Putative Phosphorylation Site. *Gene* **262**:301-307.

Hyde RJ, Cass C E, Young J D and Baldwin S A (2001) The ENT Family of Eukaryote Nucleoside and Nucleobase Transporters: Recent Advances in the Investigation of Structure/Function Relationships and the Identification of Novel Isoforms. *Mol Membr Biol* **18**:53-63.

King AE, Ackley M A, Cass C E, Young J D and Baldwin S A (2006) Nucleoside Transporters:

From Scavengers to Novel Therapeutic Targets. *Trends Pharmacol Sci* **27**:416-425.

Kiss A, Farah K, Kim J, Garriock R J, Drysdale T A and Hammond J R (2000) Molecular Cloning and Functional Characterization of Inhibitor- Sensitive (MENT1) and Inhibitor-Resistant (MENT2) Equilibrative Nucleoside Transporters From Mouse Brain. *Biochem J* **352 Pt 2**:363-372.

Kwong FYP, Wu J-S R, Shi M M, Fincham H E, Davies A, Henderson P J F, Baldwin S A and Young J D (1993) Enzymic Cleavage As a Probe of the Molecular Structures of Mammalian Equilibrative Nucleoside Transporters. *J Biol Chem* **268**:22127-22134.

Paterson ARP and Oliver J M (1971) Nucleoside Transport. II. Inhibition by P-Nitrobenzylthioguanosine and Related Compounds. *Can J Biochem* **49**:271-274.

Shi MM, Wu J-S R, Lee C-M and Young J D (1984) Nucleoside Transport: Photoaffinity Labelling of High-Affinity Nitrobenzylthioinosine Binding Sites in Rat and Guinea Pig Lung. *Biochem Biophys Res Commun* **118**:594-600.

Stolk M, Cooper E, Vilk G, Litchfield D W and Hammond J R (2005) Subtype-Specific Regulation of Equilibrative Nucleoside Transporters by Protein Kinase CK2. *Biochem J* **386**:281-289.

Valdes R, Liu W, Ullman B and Landfear S M (2006) Comprehensive Examination of Charged Intramembrane Residues in a Nucleoside Transporter. *J Biol Chem* **281**:22647-22655.

Vickers MF, Mani R S, Sundaram M, Hogue D L, Young J D, Baldwin S A and Cass C E (1999)

Functional Production and Reconstitution of the Human Equilibrative Nucleoside Transporter (HENT1) in Saccharomyces Cerevisiae. Interaction of Inhibitors of Nucleoside Transport With Recombinant Hent1 and a Glycosylation-Defective Derivative (Hent1/N48q). *Biochem J* **339**:21-32.

Visser F, Baldwin S A, Isaac R E, Young J D and Cass C E (2005a) Identification and Mutational Analysis of Amino Acid Residues Involved in Dipyridamole Interactions With Human and Caenorhabditis Elegans Equilibrative Nucleoside Transporters. *J Biol Chem*. **280**:11025-11034

Visser F, Sun L, Damaraju V, Tackaberry T, Peng Y, Robins M J, Baldwin S A, Young J D and Cass C E (2007) Residues 334 and 338 in Transmembrane Segment 8 of Human Equilibrative Nucleoside Transporter 1 Are Important Determinants of Inhibitor Sensitivity, Protein Folding and Catalytic Turnover. *J Biol Chem*. **282**:14148-14157

Visser F, Zhang J, Raborn R T, Baldwin S A, Young J D and Cass C E (2005b) Residue 33 of Human Equilibrative Nucleoside Transporter 2 Is a Functionally Important Component of Both the Dipyridamole and Nucleoside Binding Sites. *Mol Pharmacol*. **67**:1291-1298

Vyas S, Ahmadi B and Hammond J R (2002) Complex Effects of Sulfhydryl Reagents on Ligand Interactions With Nucleoside Transporters: Evidence for Multiple Populations of ENT1 Transporters With Differential Sensitivities to N-Ethylmaleimide. *Arch Biochem Biophys* **403**:92-102.

Wu SK, Ann D K, Kim K J and Lee V H (2005) Fine Tuning of Rabbit Equilibrative Nucleoside Transporter Activity by an Alternatively Spliced Variant. *J Drug Target* **13**:521-533.

Yao SY, Ng A M, Muzyka W R, Griffiths M, Cass C E, Baldwin S A and Young J D (1997) Molecular Cloning and Functional Characterization of Nitrobenzylthioinosine (NBMPR)-Sensitive (Es) and NBMPR-Insensitive (Ei) Equilibrative Nucleoside Transporter Proteins (RENT1 and RENT2) From Rat Tissues. *J Biol Chem* **272**:28423-28430.

Young JD, Jarvis S M, Robins M J and Paterson A R P (1983) Photoaffinity Labeling of the Human Erythrocyte Nucleoside Transporter by N6-(p-Azidobenzyl)Adenosine and Nitrobenzylthioinosine: Evidence That the Transporter Is a Band 4.5 Polypeptide. *J Biol Chem* **258**:2202-2208.

Zhang J, Visser F, King K M, Baldwin S A, Young J D and Cass C E (2007) The Role of Nucleoside Transporters in Cancer Chemotherapy With Nucleoside Drugs. *Cancer Metastasis Rev*. **26**:85-110

Footnotes

This study was supported by a Discovery Grant to JRH from the Natural Sciences and Engineering Research Council of Canada. KR gratefully acknowledges the financial support provided by the Schulich School of Medicine and Dentistry, University of Western Ontario, during the course of his graduate studies. DBJB is the recipient of an Ontario Graduate Scholarship in Science and Technology.

A preliminary report of this work was presented at the XVth World Congress of Pharmacology in Beijing, China, July 2007 (Acta Pharmacologica Sinica, Volume 27, Suppl 1)

Reprint requests to be sent to: Dr James R Hammond, Dept of Physiology and Pharmacology, M266 Med Sci Bldg, University of Western Ontario, London, Ontario, Canada N6A 5C1

1. Current Address: Department of Pharmaceutical Sciences, Faculty of Pharmacy, University of Toronto, 19 Russell St., Toronto, ON M5S 2S2, Canada

Molecular Pharmacology Fast Forward. Published on April 15, 2008 as DOI: 10.1124/mol.107.041871
This article has not been copyedited and formatted. The final version may differ from this version.

Figure Legends

Figure 1: Predicted topology of mENT1Δ11. The sequence is identical to mENT1 from the N-terminal to Gly356. Residues 357-361 are unique to mENT1Δ11, and residues 362-458 of mENT1 are missing from mENT1Δ11.

Figure 2: Western blots of mENT1 and mENT1Δ11. U2-OS cells were transiently transfected with either 3XFLAG-mENT1, 3XFLAG-mENT1Δ11, or the empty 3XFLAG-CMV10 vector, and membranes prepared from these cells were electrophoresed on 12% SDS-polyacrylamide gels and transferred to PVDF membranes. The blots were incubated with primary polyclonal rabbit anti-FLAG (1:1000) antibody for 2 hrs, followed by polyclonal goat anti-rabbit antibody conjugated to horseradish peroxidase (1:5000) for 1 hr. The data shown are representative of two independent experiments.

Figure 3: Tissue distribution of mENT1 and mENT1Δ11. A) RT-PCR of ENT1 and ENT1Δ11 from the indicated mouse tissues was performed using oligonucleotide primers spanning the coding region of mENT1. The mENT1Δ11 transcript (lower band) is 1250bp in size compared to the 1500 bp full-length mENT1 (upper band) on 2.0% agarose gels stained with ethidium bromide. Data shown are representative of three independent RT-PCR reactions using tissues from different mice. B) Immunoblots obtained using anti-mENT1antibody in brain (B), liver (L), pancreas (P) and testis (T) tissue homogenates. The predicted sizes of mENT1 and mENT1Δ11 are 50 kDa and 40 kDa, respectively.

Figure 4: Binding of [^{3}H]NBMPR to PK15 cells transfected with mENT1 or mENT1Δ11 without (Panel A) and with (Panel B) a FLAG-epitope tag on the N-terminus. Cells expressing mENT1 (closed symbols) or mENTΔ11 (open symbols) were incubated with a range of concentrations of

Molecular Pharmacology Fast Forward. Published on April 15, 2008 as DOI: 10.1124/mol.107.041871
This article has not been copyedited and formatted. The final version may differ from this version.

[^{3}H]NBMPR (abscissa) in the presence (nonspecific binding, circles) and absence (total binding, squares) of 10 μM NBTGR. Each point represents the mean ± SEM of the number of NBMPR binding sites per cell (ordinate) from five independent experiments conducted in duplicate.

Figure 5: Photoaffinity labelling of PK15-mENT1 and PK15-mENT1Δ11 membrane proteins with [^{3}H]NBMPR. PK15-mENT1 and PK15-mENT1Δ11 cell membranes were incubated, in parallel, with 50 nM [^{3}H]NBMPR for 1hr on ice and then exposed to UV light (~365nm) and separated on SDS-PAGE gels as described in the text. The amount of radioactivity associated with each 2 mm gel slice (dpm) are plotted against the gel migration distance and compared to a set of protein standards as shown at the top of the figure. Data shown are representative of five independent experiments.

Figure 6: [^{3}H]2-Chloroadenosine and [^{3}H]uridine uptake by PK15-mENT1 (closed symbols) and PK15-mENT1Δ11 (open symbols) cells. Cells were incubated with 10 μM [^{3}H]2-chloroadenosine (Panel A) or 100 μM [^{3}H]uridine (Panel B) for the times indicated (abscissa) in the presence (nonmediated uptake; circles) or absence (total uptake; squares) of 8 μM dipyridamole/NBTGR. Each point represents the mean ± SEM of the cellular accumulation of [^{3}H]substrate (pmol/μl of total cell water) at each time point from at least 5 independent experiments conducted in duplicate. Panel C shows the initial rate of transporter-mediated (total - nonmediated) uptake of a range of concentrations of [^{3}H]2-chloroadenosine in both the PK15-mENT1 and PK15-mENT1Δ11 cells. Each point represents the mean ± SEM from five independent experiments.

Figure 7: Inhibition of [^{3}H]2-chloroadenosine uptake by inhibitors and substrates of mENT1. PK15-mENT1 (■) and PK15-mENT1Δ11 (○) cells were incubated with 10 μM [^{3}H]2-

Molecular Pharmacology Fast Forward. Published on April 15, 2008 as DOI: 10.1124/mol.107.041871
This article has not been copyedited and formatted. The final version may differ from this version.

chloroadenosine for 15 sec in the presence and absence of the indicated concentrations of test agents. Each point represents the mean ± SEM from at least 4 independent experiments conducted in duplicate.

Figure 8: Effect of NEM on [^{3}H]NBMPR binding (upper panels) and [^{3}H]2-chloroadenosine uptake (lower panels) in PK15 cells transfected with either 3xFLAG-mENT1 (left panels) or 3xFLAG-mENT1Δ11 (right panels). Panel A, B: Cells, with (□) and without (■) pretreatment with 300 μM NEM, were incubated with a range of concentrations of [^{3}H]NBMPR in the presence and absence of 10 μM NBTGR to determine the amount of specific binding to ENT1. Results are represented as Scatchard plots (Bound versus Bound/Free) with each point being the mean of 5 independent experiments. Panel C,D: Cells, with (□) and without (■) pretreatment with 300 μM NEM, were incubated with a range of concentrations of [^{3}H]2-chloroadenosine in the presence and absence of 10 μM dipyridamole/NBMPR to determine the amount of transporter-mediated uptake of [^{3}H]2-chloroadenosine. Each point represents the mean ± SEM of the initial rate of [^{3}H]2-chloroadenosine uptake at each concentration from five independent experiments conducted in duplicate.

Molecular Pharmacology Fast Forward. Published on April 15, 2008 as DOI: 10.1124/mol.107.041871
This article has not been copyedited and formatted. The final version may differ from this version.

Table 1 : PCR Primer Sequences

Primer Name	**Sequence (5' to 3')**
5'mENT1	GCA AGA GCC AGA GGG AGG GAG
3'mENT1-Kpn1	CTT GTT AAG GGC ACT TGT GTG AGG TAC CCG GC
5'HindIII-mENT1	GGC CAA GCT TAT GAC AAC CAG T
5'hENT1	GGG AAC TAG TAG AAC ACC ATC ACC ATG ACA AC
3'hENT1	TCC TTC CTG TTC CGG GCA ATT GTA TCG ATA A

The restriction enzyme recognition sequence is underlined. Primers names beginning with 5' are the forward primers, and those beginning with 3' are the reverse primers.

Molecular Pharmacology Fast Forward. Published on April 15, 2008 as DOI: 10.1124/mol.107.041871
This article has not been copyedited and formatted. The final version may differ from this version.

Table 2 - Comparison of the functional characteristics of mENT1 and mENT1Δ11

	mENT1	mENT1Δ11
[^{3}H]NBMPR Binding		
K_d (nM)	0.19 ± 0.02	0.14 ± 0.02
B_{max} (sites/cell)	592,000 ± 16,000	600,000 ± 21,000
[^{3}H]2-Chloroadenosine Uptake		
K_m (μM)	43 ± 12	66 ± 22
V_{max} (pmol/μl/s)	4.4 ± 1.7	3.5 ± 1.1
Inhibitor Affinity (K_i)		
NBMPR (nM)	0.45 ± 0.16	0.94 ± 0.47
Dipyridamole (nM)	17 ± 8	9 ± 3
Dilazep (nM)	7.2 ± 2.0	14 ± 8
Draflazine (nM)	0.8 ± 0.3	1.0 ± 0.5
Adenosine (μM)	4.7 ± 2.0	2.6 ± 1.1
Uridine (μM)	213 ± 45	165 ± 71

Each value is the mean ± SEM from at least 4 independent experiments.

Molecular Pharmacology Fast Forward. Published on April 15, 2008 as DOI: 10.1124/mol.107.041871
This article has not been copyedited and formatted. The final version may differ from this version.

TABLE 3 - Effect of NEM on NBMPR binding and 2-chloroadenosine uptake by PK15 cells transfected with mENT1 or mENT1Δ11

	mENT1		mENT1Δ11	
	Control	NEM	Control	NEM
NBMPR binding				
K_d1 (nM)	0.15 ± 0.01	0.53 ± 0.15*	0.021 ± 0.005	0.025 ± 0.008
K_d2 (nM)	-	-	1.9 ± 0.9	0.61 ± 0.07*
B_{max}1 (sites/cell)	517000 ± 111000	725000 ± 128000*	134000 ± 40000	55,000 ± 20000*
B_{max}2 (sites/cell)	-	-	546000 ± 146,000	602000 ± 133000
2-Chloroadenosine Uptake				
K_m (μM	44 ± 19	95 ± 34*	43 ± 11	55 ± 16
V_{max} (pmol/μl/s)	17 ± 4	27 ± 4*	19 ± 3	18 ± 4

* indicates a significant difference from the respective control (Student's t-test for paired samples, $P < 0.05$). Each value is the mean ± SEM from at least 4 independent experiments.

Figure 1

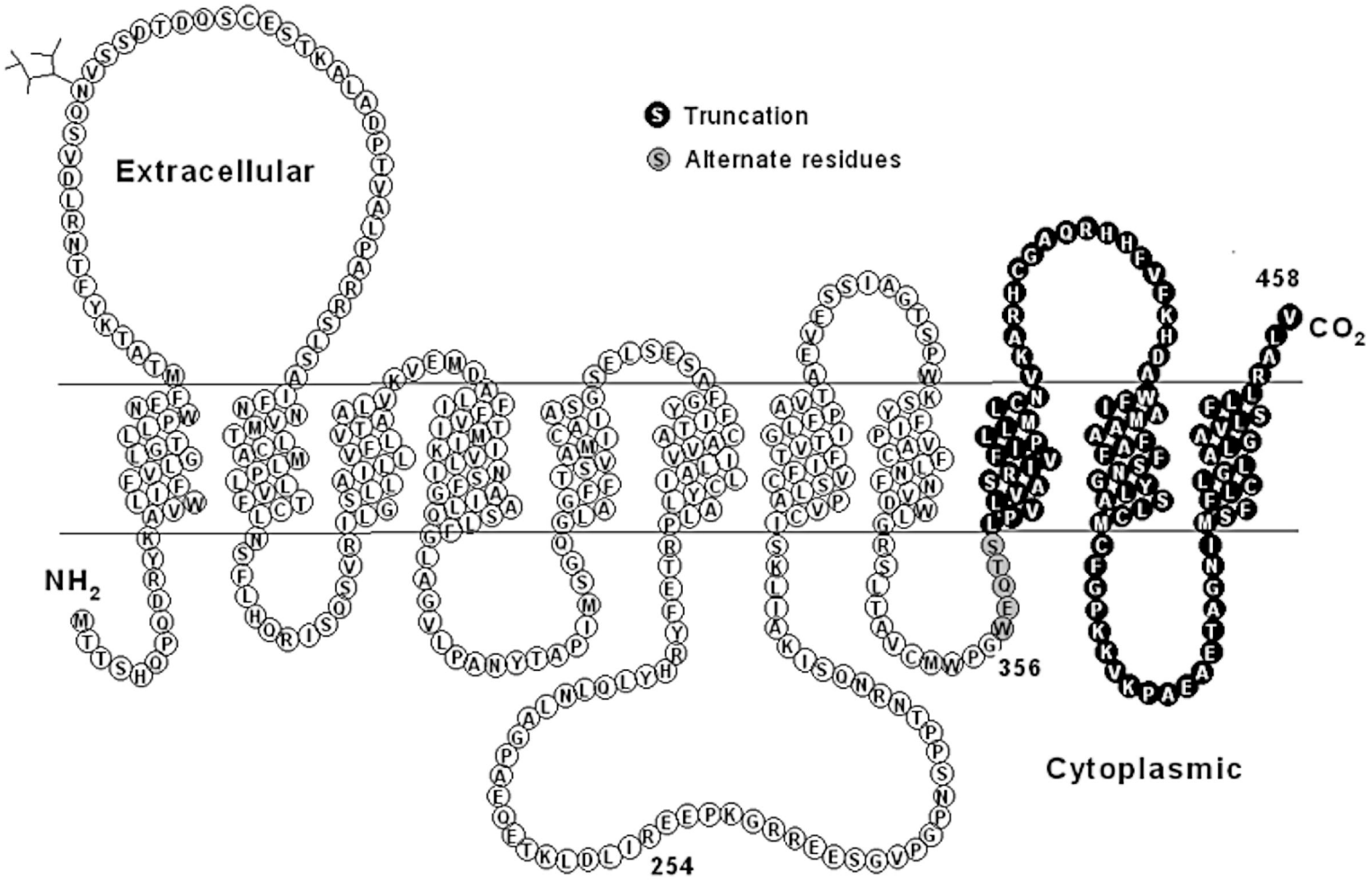
Truncation
Alternate residues
Extracellular
Cytoplasmic
NH2
CO2
458
356
254

Figure 2

Figure 3

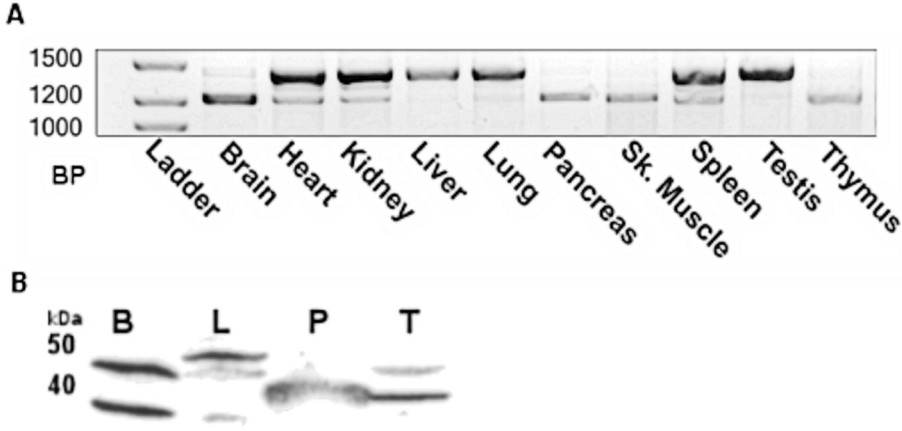
A
1500
1200
1000
BP
Ladder
Brain
Heart
Kidney
Liver
Lung
Pancreas
Sk. Muscle
Spleen
Testis
Thymus
B
kDa
50
40
B
L
P
T

Figure 4

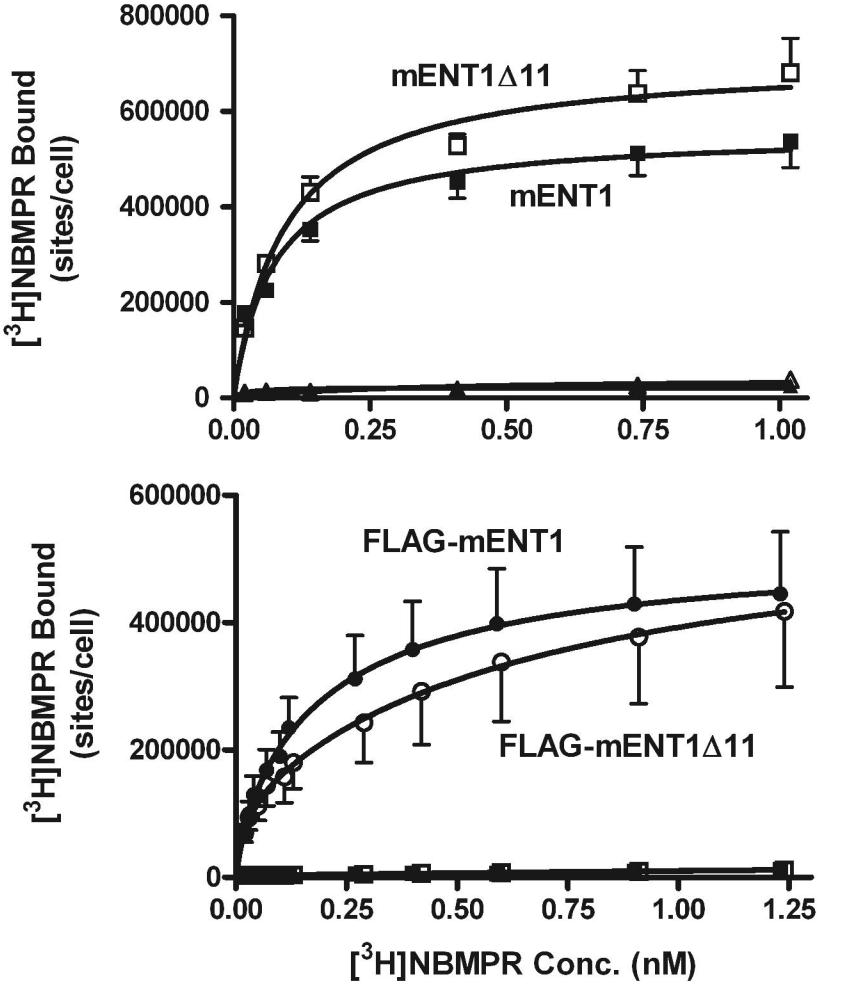
800000
600000
400000
200000
0
[3H]NBMPR Bound (sites/cell)
mENT1Δ11
mENT1
0.00
0.25
0.50
0.75
1.00
600000
400000
200000
0
FLAG-mENT1
FLAG-mENT1Δ11
0.00
0.25
0.50
0.75
1.00
1.25
[3H]NBMPR Conc. (nM)

Figure 5

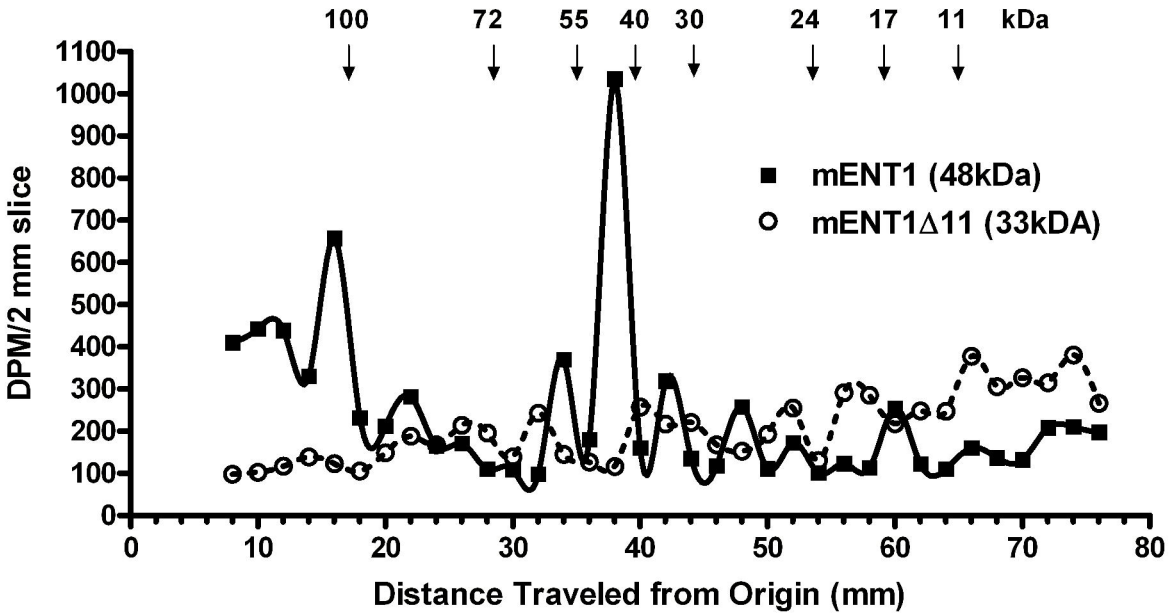
100
72
55
40
30
24
17
11
kDa
1100
1000
900
800
700
600
500
400
300
200
100
0
DPM/2 mm slice
mENT1 (48kDa)
mENT1Δ11 (33kDA)
0
10
20
30
40
50
60
70
80
Distance Traveled from Origin (mm)

Figure 6

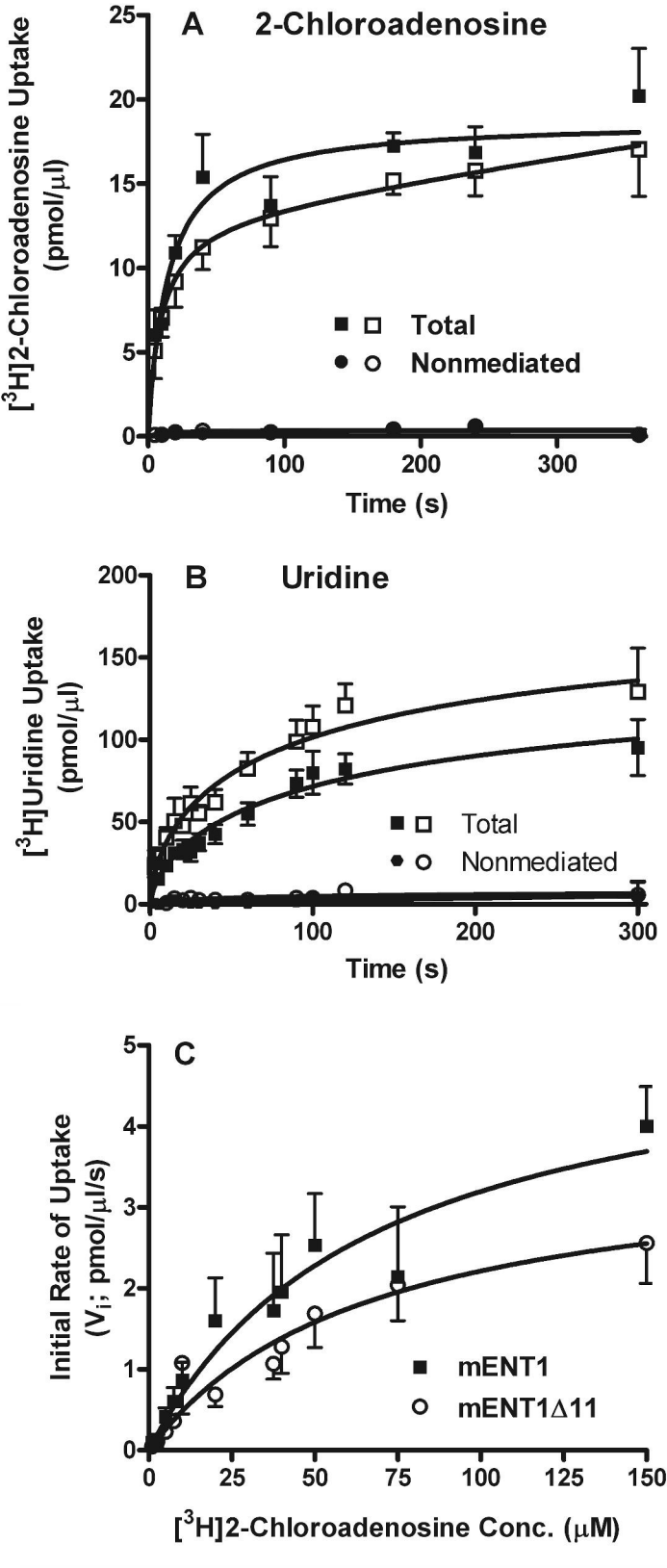
A
2-Chloroadenosine
[3H]2-Chloroadenosine Uptake (pmol/μl)
Total
Nonmediated
Time (s)
B
Uridine
[3H]Uridine Uptake (pmol/μl)
Total
Nonmediated
Time (s)
C
Initial Rate of Uptake (Vi; pmol/μl/s)
mENT1
mENT1Δ11
[3H]2-Chloroadenosine Conc. (μM)

Figure 7

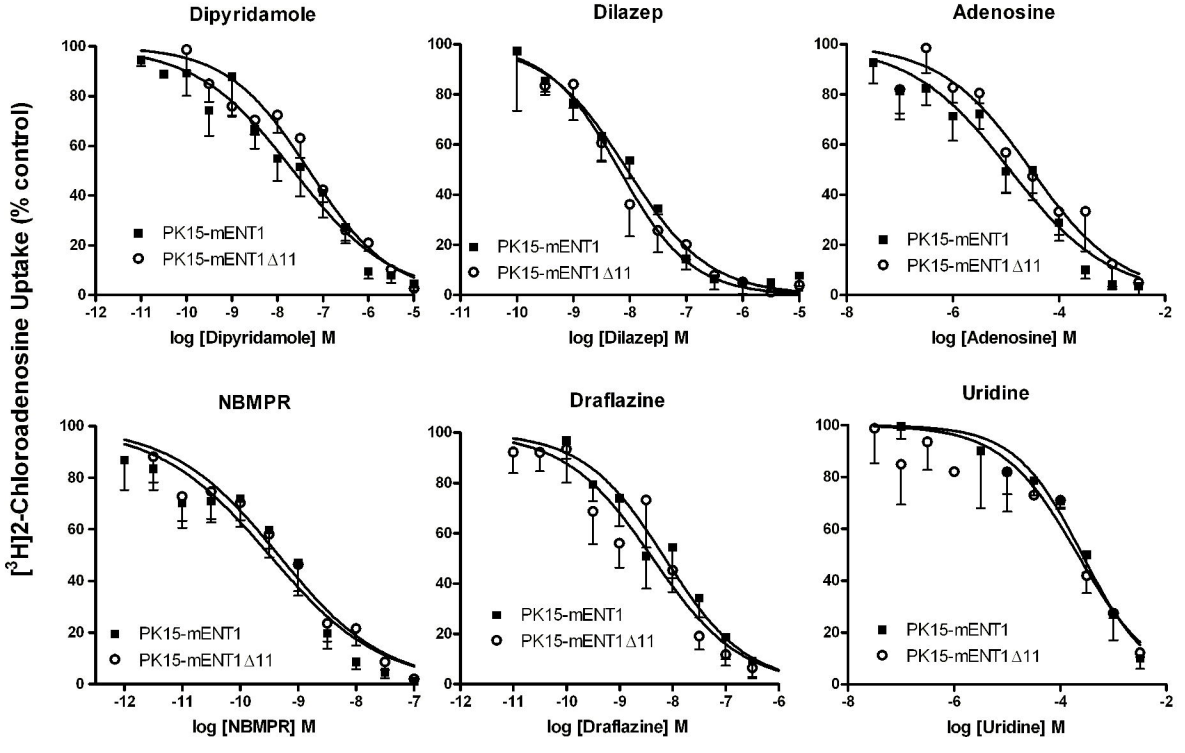
Dipyridamole
Dilazep
Adenosine
NBMPR
Draflazine
Uridine
[3H]2-Chloroadenosine Uptake (% control)
PK15-mENT1
PK15-mENT1Δ11
log [Dipyridamole] M
log [Dilazep] M
log [Adenosine] M
log [NBMPR] M
log [Draflazine] M
log [Uridine] M

Figure 8

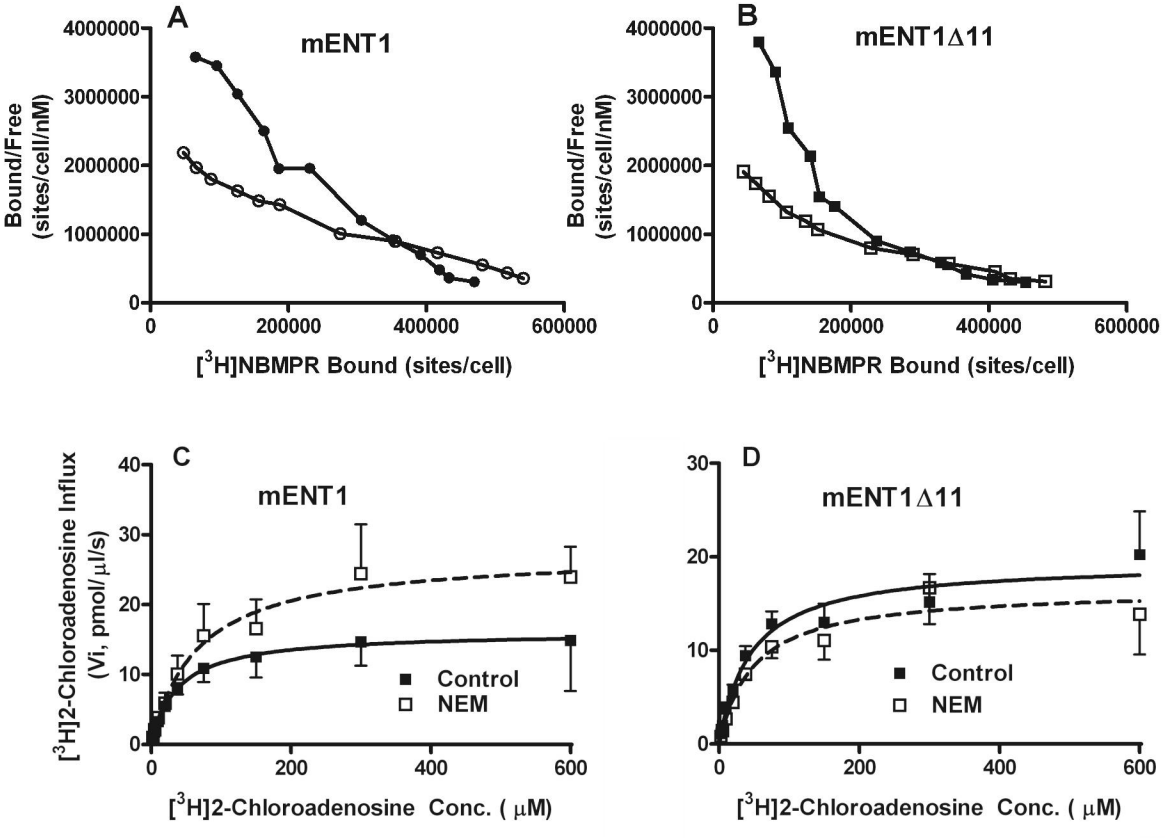
A
mENT1
Bound/Free (sites/cell/nM)
4000000
3000000
2000000
1000000
0
0
200000
400000
600000
[3H]NBMPR Bound (sites/cell)
B
mENT1Δ11
Bound/Free (sites/cell/nM)
4000000
3000000
2000000
1000000
0
0
200000
400000
600000
[3H]NBMPR Bound (sites/cell)
C
mENT1
[3H]2-Chloroadenosine Influx (Vi, pmol/μl/s)
40
30
20
10
0
Control
NEM
0
200
400
600
[3H]2-Chloroadenosine Conc. (μM)
D
mENT1Δ11
30
20
10
0
Control
NEM
0
200
400
600
[3H]2-Chloroadenosine Conc. (μM)